Available online at www.sciencedirect.com
ScienceDirect
Energy 32 (2007) 1260–1270
ENERGY
www.elsevier.com/locate/energy

Effect of flow maldistribution on thermal performance of a solar air heater array with subcollectors in parallel

Rajendra Karwa[a,*], Nitin Karwa[b], Rohit Misra[c], P.C. Agarwal[c]

[a]Department of Mechanical Engineering, Faculty of Technology, Addis Ababa University, P.O. Box 385, Addis Ababa, Ethiopia
[b]Department of Mechanical Engineering, Indian Institute of Technology, Delhi 110 016, India
[c]Department of Mechanical Engineering, Faculty of Engineering, Jai Narain Vyas University, Jodhpur 342 011, India

Received 11 October 2004

Abstract

This paper presents results of a theoretical study carried out to investigate the effect of flow maldistribution, caused by the manufacturing imperfections and tolerances, on the thermal efficiency of a solar air heater array with subcollectors in parallel. The air mass flow rate, ambient temperature, solar insolation and wind heat transfer coefficient have been systematically varied to study the effect under a wide range of these parameters. The collector length, duct height, and plate emissivity were also changed to study their effect. It has been found that the maximum reduction in thermal efficiency due to flow maldistribution is less than about 3% for an array with a commercial grade finish of duct surfaces and $\pm 10\%$ manufacturing tolerance for the duct height.

Keywords: Solar air heater array; Subcollectors in parallel; Flow imbalance; Thermal performance

1. Introduction

The collectors in a solar air heater array are often arranged so that the air flows through the collectors in series, parallel, or combined series and parallel mode. Yeh and Lin [1], and Garg and Adhikari [2] showed that the thermal efficiency (ratio of the useful heat gain and the incident solar radiation on the air heater plane) of an array can be improved by operating several subcollectors with identical collector aspect ratios (ratio of collector length to width, L/W) in a series in place of a single large collector with the same total area. A collector module in an array is termed as subcollector of the array. It is to be noted that N-subcollectors in a series basically constitute a high aspect ratio collector while the parallel arrangement of N-subcollectors is equivalent to a low aspect ratio collector. Thus, it is evident that the improvement in the thermal efficiency obtained [1,2] for a number of subcollectors in a series is the result of a decrease in the cross-sectional area of the air duct. This increases the velocity of air and, hence, increases the convective heat transfer rate from the absorber plate to the air flowing through the duct. However, these studies did not consider the effect of the configuration change on the pressure drop through the duct and the pumping power required for propelling the air. Recently, Karwa et al. [3] carried out a thermo-hydraulic performance evaluation of the solar air heater arrays (subcollectors arranged in a series, parallel or combined series and parallel mode) using a mathematical model. Based on the performance evaluation criterion of equal pumping power, they have shown that an array with subcollectors in parallel is about 3–33% better in thermal efficiency than the array with subcollectors in a series.

Jones and Lior [4,5] studied the effect of the ratio of tube diameter to manifold diameter, the number of tubes, and the length of the tubes on flow maldistribution in solar water heaters with a vertical orientation of the tubes. In general, they found that the flow-starved tubes would become warmer than other tubes and this causes the onset of natural convection inside the flow-starved tubes (the buoyancy-driven flow). The buoyancy effect tends to diminish the flow maldistribution to some extent. The results of their study further showed that for the tube-to-manifold

*Corresponding author. Tel.: +251 1 639016; fax: +251 1 239480.
E-mail address: karwa_r@yahoo.com (R. Karwa).

0360-5442/$ - see front matter © 2006 Elsevier Ltd. All rights reserved.
doi:10.1016/j.energy.2006.08.002

Nomenclature

A	absorber plate area (m^2)
c_p	specific heat of air ($J\,kg^{-1}\,K^{-1}$)
D_h	hydraulic diameter of duct $= 4WH/[2(W+H)]$ (m)
e/D_h, e/D	relative roughness
f	Fanning friction factor
f_{app}	apparent friction factor in the entry region
F_R	heat removal factor
G	nominal mass flow rate per unit area of absorber plate $= m/WH$ ($kg\,s^{-1}\,m^{-2}$)
h	heat transfer coefficient from absorber plate to air ($W\,m^{-2}\,K^{-1}$)
h_w	wind heat transfer coefficient ($W\,m^{-2}\,K^{-1}$)
H	nominal duct height (m)
I	solar radiation intensity ($W\,m^{-2}$)
k	thermal conductivity of air ($W\,m^{-1}\,K^{-1}$)
L	length of collector (m)
L/W	collector aspect ratio
m	mass flow rate ($kg\,s^{-1}$)
N	number of subcollectors in parallel
Nu	Nusselt number $= hD_h/k$
P	pumping power (W)
Pr	Prandtl number
Q	heat collection rate (W)
Q_L	heat loss from collector (W)
Re	Reynolds number
T_a	ambient temperature (K)
T_i	inlet air temperature (K)
T_m	mean air temperature $= (T_i+T_o)/2$ (K)
T_{mpg}	mean of the plate and glass temperatures $= (T_p+T_{gi})/2$ (K)
T_o	outlet air temperature (K)
T_p	mean plate temperature (K)
T_s	sky temperature (K)
U_L	overall loss coefficient ($W\,m^{-2}\,K^{-1}$)
W	width of the duct (m)
W/H	duct aspect ratio

Greek symbols

δp	pressure drop (Pa)
δ_{pg}	gap between the absorber plate and glass cover (m)
β	collector slope (deg)
ε_g	emissivity of glass
ε_p	emissivity of plate
η	thermal efficiency of array
μ	dynamic viscosity of air (Pa s)
ν_{mpg}	kinematic viscosity of air at temperature T_{mpg} ($m^2\,s^{-1}$)
ρ	density of air ($kg\,m^{-3}$)
σ	Stefan–Boltzmann constant $= 5.67\times10^{-8}$ ($W\,m^{-2}\,K^{-4}$)
$\tau\alpha$	transmittance–absorptance product

diameter ratios of 0.25 and smaller, the flow is nearly uniformly distributed in the tubes and there is a negligible influence of buoyancy. In fact, a small value of tube-to-manifold diameter ratio causes higher pressure drops in the tubes relative to that in the manifold. Weitbrecht et al. [6] concluded from their study on a flat plate solar water heater that the flow distribution depends on the relation between ratio of energy (pressure) loss in the risers and energy losses in the manifolds, and to obtain a homogeneous flow distribution the influence of the energy losses in the risers must control the system. Hence, it can be inferred from these studies that the flow distribution will tend towards uniformity when the pressure drops in the ducts of a solar air heater array become large relative to that in the manifold and in such a situation the buoyancy effect can be neglected. Shah and Sekulic [7] have also suggested that for the properly designed manifolds, their effect on the flow distribution in parallel flow passages of heat exchangers is not significant.

In general, the flow maldistribution leads to a lower rate of energy collection in the subcollectors with low flow rates [8,9]. However, Culham and Sauer [9] found that the flow maldistribution has only a marginal effect on the total energy collection in case of water heaters, provided that the flow rate in the collector riser tubes is 35% or more of the nominal value with a pressure drop across the riser at least 10 times greater than the drop across the headers. Based on the study of Culham and Sauer, Karwa et al. [3] assumed a uniform energy collection in the parallel paths of the solar air heater array in their analysis. Such assumption is worth investigation because the thermohydraulic behaviour of the fluids in the solar water and air heaters is not the same.

In case of an array with subcollectors in parallel (Fig. 1), differences in duct heights and surface finish of the ducts as a result of the manufacturing imperfections and tolerances can cause the flow maldistribution as explained below.

The surfaces of the parallel air flow ducts in an array may range from smooth to commercially finished [10]. The relative roughness, e/D_h, of a surface with commercial grade finish is of the order of 0.002.

Friction factor correlation for flow in a roughened circular duct due to Zigrang and Sylvester [Table 4.3 in 11], for $2800 \leqslant Re \leqslant 10^8$, $4\times10^{-8} \leqslant e/D \leqslant 0.1$, is

$$1/\sqrt{f} = 3.4769 - 1.7372 \times \ln[(2e/D) - (16.1332/Re)\ln A_1], \quad (1)$$

where $A_1 = [(2e/D)/7.4 + 13/Re]$ and e/D is the relative roughness.

From the above correlation it can be seen that the friction factor of a circular duct with relative roughness of 0.002 is higher by about 4–11% than the smooth surfaced

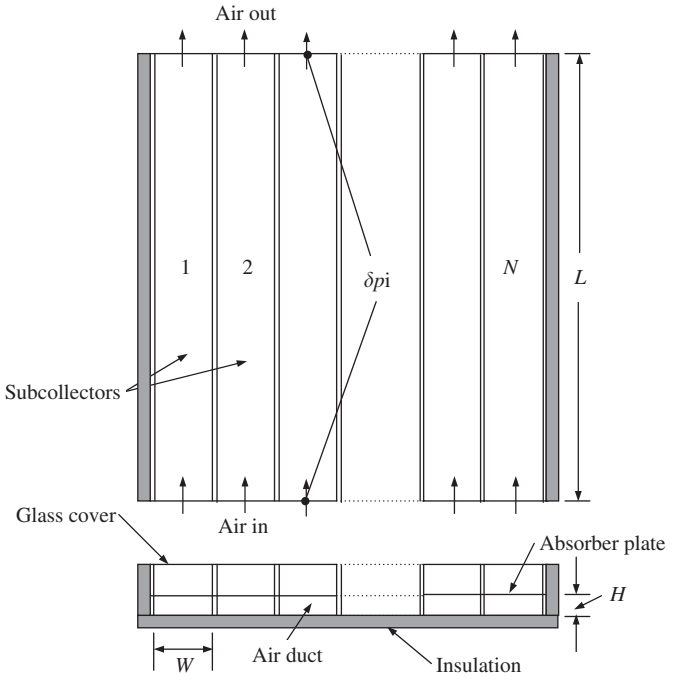

Fig. 1. Solar air heater array with N-subcollectors in parallel.

duct in the Reynolds number range of 2800–14,000; the greater increase is at the higher Reynolds number.

Equation of pressure loss can be transformed as under for the high aspect ratio ($W \gg H$) rectangular cross-section duct of a solar air heater ($D_h \approx 2H$) [3]

$$\begin{aligned}\delta p &= [(4fL)/(2\rho D_h)](m/WH)^2 \\ &= (4fL)/(4\rho H)[(WLG)/(WH)]^2 \\ &= (fG^2/\rho)(L/H)^3. \end{aligned} \quad (2)$$

The available pressure drop across each duct in an array with subcollectors in parallel is established by the pressure distribution in the manifolds as shown by Jones and Lior [5] for the tubes of a vertical solar water heater. Thus it can be seen from Eq. (2) that a decrease in the height of the duct of a subcollector will lead to a reduced air flow rate which will lead to a proportionate decrease in the Reynolds number. In the laminar flow regime, the friction factor is not affected due to the wall roughness but a decrease in the Reynolds number will increase the friction factor. For the flow in the transition and turbulent regime, though the friction factor is not affected as much as in the laminar regime due to the decrease in the Reynolds number, the surface roughness may significantly increase the friction factor. The combined effect of the decrease in the duct height of a subcollector in the array, the increase in the friction factor due to the reduced Reynolds number, and wall roughness will cause an enhanced flow resistance. Hence, a subcollector with manufacturing imperfections (smaller than nominal duct height and surface roughness) will have lower flow rate than a smooth duct subcollector of nominal duct height in an array.

It can be inferred from the above discussion that the flow maldistribution in parallel ducts of an array can be manifold induced, may be due to the duct-to-duct variations because of manufacturing tolerances and imperfections, and may be affected due to the buoyancy. However, the studies for solar water heaters with vertical tubes have shown that the flow distribution in the parallel tubes is only marginally affected due to the manifolds and buoyancy when the pressure drop in the tubes is large relative to that in the manifolds. This conclusion must also be true for a solar air heater array. Hence, the basic objective of the present theoretical study is to investigate the effect of flow maldistribution, caused by the manufacturing imperfections and tolerances of the ducts, on the thermal performance of a solar air heater array with subcollectors in parallel.

2. Mathematical model

The effect of the flow maldistribution on the thermal performance of an array with subcollectors in parallel has been evaluated by following an iterative process using a non-linear mathematical model presented below.

The energy balance of a solar air heater gives the distribution of incident solar energy, I, into energy gain, Q, and various losses. It is given by

$$\begin{aligned} Q &= A[I(\tau\alpha) - U_L(T_p - T_a)] \\ &= AF_R[I(\tau\alpha) - U_L(T_i - T_a)], \end{aligned} \quad (3)$$

where A is the area of the absorber plate receiving the solar insolation and product $(\tau\alpha)$ is the transmittance–absorptance product of the cover–absorber plate combination. Factor F_R in Eq. (3) is termed as heat removal factor [12].

The energy gain of the solar air heater equals the heat transferred to the air flowing through the duct of the collector and is given by

$$Q = mc_p(T_o - T_i) = GAc_p(T_o - T_i). \quad (4)$$

The convective heat transfer equation gives

$$Q = hA(T_p - T_m). \quad (5)$$

The term T_p is the mean absorber plate temperature and T_m is the mean air temperature. U_L in Eq. (3) is known as overall loss coefficient of a solar collector and is given by

$$U_L = Q_L/[A(T_p - T_a)], \quad (6)$$

where Q_L is the overall heat loss. It is a sum of heat losses from the top, Q_t, the back, Q_b, and the edge, Q_e.

Since the use of the empirical equations of the top loss can lead to a significant error in it's estimate [13], the present model estimates this loss from the basic heat transfer equations.

From absorber plate to inner surface of the glass cover, the heat transfers by radiation and convection, hence,

$$Q_{tpg} = A\left[\sigma\left(T_p^4 - T_{gi}^4\right)(1/\varepsilon_p + 1/\varepsilon_g - 1)^{-1} + h_{pg}(T_p - T_{gi})\right]. \quad (7)$$

The equation for the conduction heat transfer through the glass is

$$Q_{tg} = k_g A(T_{gi} - T_{go})/\delta_g, \quad (8)$$

where k_g and δ_g are the thermal conductivity and thickness of the glass, respectively.

From the outer surface of the glass, the heat is rejected by radiation and convection to the ambient, hence,

$$Q_{tga} = A\left[\sigma\varepsilon_g\left(T_{go}^4 - T_s^4\right) + h_w(T_{go} - T_a)\right], \quad (9)$$

where T_s is the sky temperature and h_w is the wind heat transfer coefficient

In equilibrium, $Q_{tpg} = Q_{tg} = Q_{tga} = Q_t$.

The convective heat transfer coefficient between the absorber plate and glass cover, h_{pg}, has been estimated from the following three-region correlation of Buchberg et al. [14]

$$Nu = 1 + 1.446(1 - 1708/Ra')^{+} \quad \text{for } 1708 < Ra' < 5900 \quad (10a)$$

(the + bracket goes to zero when negative)

$$Nu = 0.229(Ra')^{0.252} \quad \text{for } 5900 < Ra' < 9.23 \times 10^4, \quad (10b)$$

$$Nu = 0.157(Ra')^{0.285} \quad \text{for } 9.23 \times 10^4 < Ra' < 10^6, \quad (10c)$$

where Rayleigh number for the inclined air layers, $Ra' = Ra\cos\beta$

$$Ra = GrPr,$$

$$Gr = g(T_p - T_{gi})\delta_{pg}^3 \Big/ \left(T_{mpg}\nu_{mpg}^2\right),$$

where δ_{pg} is the gap between the absorber plate and glass.

The back and edge losses, Q_b and Q_e, respectively, have been calculated from following equations [15]:

$$Q_b = A(T_p - T_a)/(\delta/k_i + 1/h_w), \quad (11)$$

$$Q_e = 0.5A_e(T_p - T_a), \quad (12)$$

where δ is the insulation thickness and k_i is the thermal conductivity of the insulation material. A_e in Eq. (12) is the area of the edge of the collector rejecting heat to the ambient.

The out let air temperature can be estimated from

$$T_o = T_i + Q/(mc_p). \quad (13)$$

The thermal efficiency estimates strongly depend on the use of appropriate heat transfer and friction factor correlations for the solar air heater ducts. These correlations must take into account the effects of the asymmetric heating encountered in the solar air heaters, duct aspect ratio and developing length, and must be applicable to the laminar to early turbulent flow regimes. The geometry of interest is the parallel plate duct (a rectangular duct of high aspect ratio) since the width of the duct is of the order of 1 m and height is of the order of 5–10 mm [3,10], with one wall at constant heat flux and the other insulated. An intensive survey of the literature has been carried out for the correlations to fulfill these requirements.

For hydrodynamically developing laminar flow in parallel plate ducts, Chen [Eqs. (5.206) and (5.207) in 16] has presented the following equations for the hydrodynamic entrance length, L_{hy}, and apparent friction factor, f_{app}, respectively,

$$L_{hy}/D_h = 0.011\,Re + 0.315/(1 + 0.0175\,Re), \quad (14)$$

$$f_{app} = 24/\mathrm{Re} + (0.64 + 38/Re)D_h/(4L). \quad (15)$$

From Eq. (14), L_{hy}/D_h is less than 30 for $Re \leqslant 2550$, while L/D_h of the subcollectors in the arrays of the present study ranges from 100 to 200. Eq. (15) takes account of the increased friction in the entrance region and the change of the momentum flux.

The thermal entrance length, L_{th}/D_h, for the laminar flow in a flat parallel plate passage, when one wall is insulated and other subjected to uniform heat flux, is of the order of $0.1(Re\ Pr)$ [17] for approach of Nusselt number value within about 1% of the fully developed Nusselt number value. For the range of present study, it extends up to about 195 hydraulic diameters. The appropriate Nusselt number–Reynolds number relation for the thermally developing laminar flow in a parallel plate duct has been presented by Hollands and Shewen [10], which has been deduced from [18] and agrees well with the data of Heaton et al. [17],

$$Nu = 5.385 + 0.148\,Re(H/L) \quad \text{for } Re < 2550. \quad (16)$$

The second term containing H/L takes the entrance length effect into account.

The friction factor correlation of Bhatti and Shah [11] for the transition to turbulent flow regime in rectangular cross-section smooth duct ($0 \leqslant H/W \leqslant 1$) is

$$f = (1.0875 - 0.1125\,H/W)f_o, \quad (17)$$

where

$$f_o = 0.0054 + 2.3 \times 10^{-8}\,Re^{1.5} \quad \text{for } 2100 \leqslant Re \leqslant 3550 \quad (17a)$$

and

$$f_o = 1.28 \times 10^{-3} + 0.1143\,Re^{-0.311} \quad \text{for } 3550 < Re \leqslant 10^7. \quad (17b)$$

They report an uncertainty of $\pm 5\%$ in the predicted friction factors from the above correlation.

The study of the apparent friction factor plots for the entrance region of a flat parallel plate duct in the turbulent flow regime presented along with those for a circular tube in [11] shows that the trend of variation in the friction factor in the entrance region for the parallel plates is not significantly different from that for a circular tube. Hence, in the present study, the following circular tube relation [11] has been used for the estimate of the apparent friction factor:

$$f_{\text{app}} = f + 0.0175(D_{\text{h}}/L). \tag{18}$$

The thermal entrance length, $L_{\text{th}}/D_{\text{h}}$, for the turbulent flow of air, based on the local Nusselt number approaching the fully developed value, ranges from 20 to 30 for the Reynolds number range of 8000–30,000 [19,20]. Kays and Leung [21] solved the fully developed turbulent-flow energy equations with constant heat rate for parallel plate duct with one side insulated. Their results are reported to be in excellent agreement with the experimental data for air [22]. The following Nusselt number correlations, deduced by Hollands and Shewen [10] from the data of Kays and Leung [21] and Tan and Charters [23] for collectors with $L/H > 125$, have been used in the present study

$$Nu = 4.4 \times 10^{-4}\, Re^{1.2} + 9.37\, Re^{0.471}(H/L) \quad \text{for } 2550 \leqslant Re \leqslant 10^4 \text{ (transition flow)} \tag{19a}$$

and

$$Nu = 0.03 Re^{0.74} + 0.788 Re^{0.74}\,(H/L) \quad \text{for } 10^4 < Re \leqslant 10^5 \text{ (early turbulent flow)}, \tag{19b}$$

where the terms containing H/L take the entrance length effect into account.

The Nusselt number data from the correlation of Hollands and Shewen for fully developed turbulent flow are in close agreement with data of Hatton et al. [24]. They are about 10% lower than the data from tube correlation of Petukhov et al. in Bhatti and Shah [11] for $Re \geqslant 8000$ and about 15–20% lower than that from $Nu = 0.023 Re^{0.8} Pr^{0.4}$ for $Re \geqslant 10{,}000$. This is in agreement with the observations of Sparrow et al. [25] in an experimental study under ideal laboratory conditions for a rectangular duct with $W/H = 5$ and $Re = 1.8 \times 10^4 - 1.42 \times 10^5$, and Tan and Charters [23] for an asymmetrically heated duct of solar air heater ($W/H = 3$; $Re = 9500$–$22{,}000$). From the close agreement of the Nusselt number data from Eq. (19b) with the results of carefully conducted experimental studies, it can be inferred that the uncertainty in the predicted Nusselt number values must be of the order of 5–6%. However, the information on the transition flow in a flat or rectangular duct is extremely sparse and a higher uncertainty in the Nusselt number values determined from Eq. (19a) may be possible. Hollands and Shewen [10] based on the information available in [18], concluded that the flow is laminar for $Re < 2550$ and turbulent for $Re > 10^4$. By analogy with the results for rectangular ducts with $W/H = 8$ [26], they concluded that power-law fits extending from the laminar result to the turbulent result would be satisfactory for the transition regime. However, the lower limit of the critical Reynolds number for a parallel plate duct is reported [16] to be 2200–3400, depending on the entrance configurations and disturbance sources. For a high aspect ratio rectangular duct with abrupt entrance, the same is reported to be 2920–3100. Hence, the laminar flow regime has been assumed up to $Re = 2800$ in the present study, which also limits the inconsistency of the predicted Nusselt number and friction factor values from the different correlations used here to about 5% at the laminar–transition interface.

Knowing the Nusselt number from the above correlations, the heat transfer coefficient, h, is found from

$$h = Nu\, k/D_{\text{h}}. \tag{20}$$

The equations for determination of pressure loss across a subcollector and pumping power are

$$\delta p = [(4fL)/(2\rho D_{\text{h}})](m/WH)^2, \tag{21}$$

$$P = (m/\rho)\delta p. \tag{22}$$

The thermal efficiency of a solar collector is defined as the ratio of the useful heat gain and the incident solar radiation on the plane of the collector. Hence, the efficiency of an array, η, is based on the heat gain of the array, which is the sum of the heat collection rates of all subcollectors in the array, i.e.,

$$\eta = \Sigma Q_i/(IA), \tag{23}$$

where Q_i is the heat collection rate of ith subcollector in the array and $i = 1$–N, and A in Eq. (23) is the total area of the absorber plates of N subcollectors in the array.

Niles et al. [27] used the following equation for the calculation of the outlet air temperature when the ambient air passes through a solar air heater (i.e., $T_{\text{i}} = T_{\text{a}}$)

$$T_{\text{o}} = T_{\text{a}} + I(\tau\alpha)\xi/U_{\text{L}}, \tag{24}$$

where $\xi = 1 - \exp[-U_{\text{L}}/(Gc_{\text{p}})(1 + U_{\text{L}}/h)^{-1}] = (F_{\text{R}} U_{\text{L}}/Gc_{\text{p}})$, and they calculated the plate temperature using the following equation:

$$T_{\text{p}} = T_{\text{i}} + [I(\tau\alpha)/U_{\text{L}}](1 - G\xi c_{\text{p}}/U_{\text{L}}). \tag{25}$$

Eqs. (24) and (25) have been used for the cross-check of the values of T_{o} and T_{p} calculated from Eqs. (3)–(23).

The transmittance–absorptance product for the absorber–cover combination is taken as 0.8 for a single glass cover. The gap between the absorber plate and glass cover is taken as 40 mm [14]. Collector slope, β, is taken as 0° (horizontal; for the ease of installation and summer operation) and 45° (the near optimum inclination for the winter operation). The thickness and thermal conductivity of the glass have been taken as 4 mm and $0.78\ \text{W m}^{-1}\,\text{K}$, respectively. Back insulation thickness is 50 mm. Thermal conductivity of the material for the back insulation is $0.037\ \text{W m}^{-1}\,\text{K}^{-1}$. Long wave emissivity values for the glass

cover and absorber plate with flat black paint have been taken as 0.88 and 0.95, respectively. The emissivity of the plate with a selective coating has been taken as 0.1. Inlet air is assumed to be at the ambient temperature of 283 K (winter operation), and 298 or 313 K (summer operation) corresponding to Western Rajasthan conditions. Solar insolation, I, has been varied from 500 $W m^{-2}$ (the lowest value) to 1000 $W m^{-2}$ (as peak value). Wind heat transfer coefficient, h_w, is taken as 5 $W m^{-2} K^{-1}$ (no wind) and 50 $W m^{-2} K^{-1}$ (corresponding to a high wind velocity). Based on the extremities of the use of a solar air heater (space heating to crop drying), the nominal mass flow rate per unit area of absorber plate, G, has been taken as 0.005–0.06 $kg s^{-1} m^{-2}$. The Reynolds number corresponding to the flow rate and collector length in this study ranges from about 200–14,000. The study considered both the assumptions of the sky temperature: $T_s = T_a$ and $T_s = 0.0552 T_a^{1.5}$ [28]. The nominal value of duct height, H, has been taken as 10 mm (high performance and high-pressure drop collector) or 20 mm for array length $L = 2$ m and 5 mm for $L = 1$ m. The width, W, of the subcollector has been fixed at 1 m while the length is either 1 or 2 m, which are the normally accepted values for a collector module from the constraints of available sizes of plywood and glass sheets, and the ease of installation and handling.

In the case of flow through a tube or in a symmetrically heated duct, an increase in the friction factor leads to the enhancement in the heat transfer coefficient (the Reynolds analogy). But a solar air heater duct has one heated and three adiabatic walls, hence, it has been assumed in the present study that the increased friction factor due to wall roughness will not lead to a proportionate increase in the heat transfer rate.

The iteration for the estimate of top loss (Eqs. (7)–(9)), has been continued till the heat loss estimates from the absorber plate to the glass cover and glass cover to the ambient differed by less than 0.2%. This affects the end result by about 0.1–0.6% only. For the heat collection estimate, the iteration was terminated when the successive values of the plate and outlet air temperatures differed by less than 0.05 K. Thermophysical properties of the air have been taken at the corresponding mean temperatures.

Sensitivity analysis shows that 1% change in the heat transfer coefficient between the absorber plate and air affects the end result (the loss in the thermal efficiency of the array) by 0.2–1.5% depending on the flow rate, while the end result is affected by 0.25–3.5% when the friction factor is changed by 1%. An error of 1% in the estimate of heat transfer coefficient between the glass cover and absorber plate has an effect of the order of 0.2–1.2% on the predicted thermal efficiency.

The mathematical model presented here has been validated against the data of the experimental study for a smooth duct solar air heater published in an earlier work of the first author [29]. The plots of thermal efficiency versus the Reynolds number in Fig. 2(a) shows that the standard deviation of predicted and experimental values is ±4.85%,

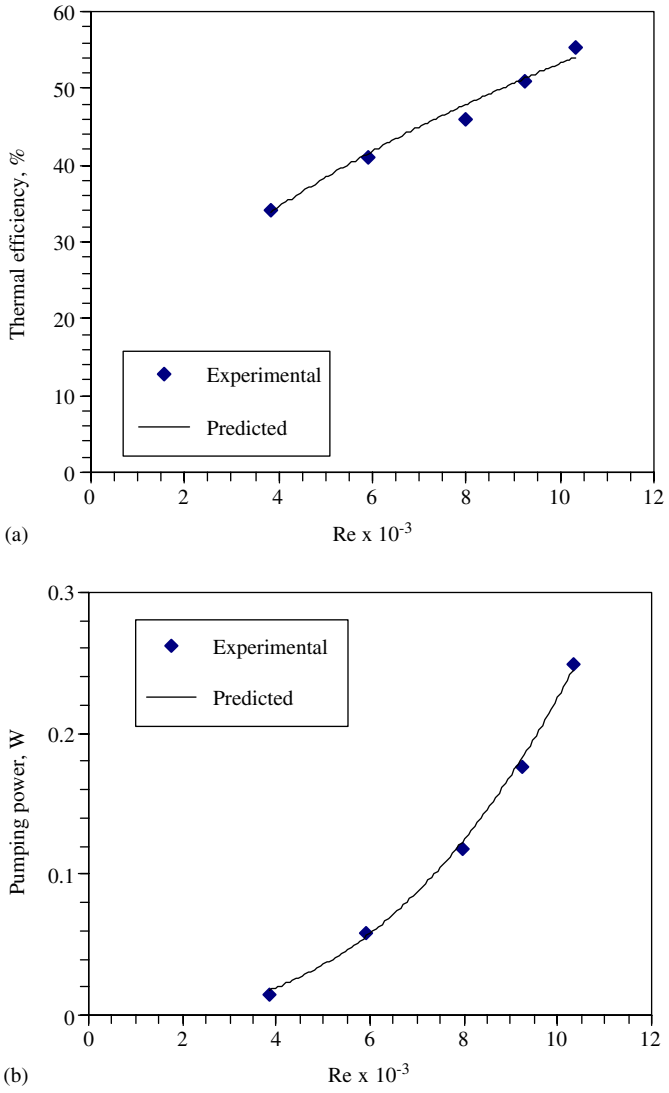

Fig. 2. Comparison of predicted values of thermal efficiency and pumping power with experimental values.

while the standard deviation of the predicted and experimental values of the pumping power in Fig. 2(b) is estimated to be ±6.15%. The good agreement between the predicted and experimental values ensures that the mathematical model can be utilized with confidence for the prediction of thermohydraulic performance of the solar air heater array.

3. Results and discussion

The effect of manufacturing imperfections on the flow distribution in the parallel ducts of subcollectors in an array has been discussed in Section 1 of this paper. To study the effect of flow maldistribution on the thermal performance of the array, four configurations, termed as basic, A, B, and C, have been considered. These configurations are listed in Table 1 and described below in detail.

In the basic configuration (refer Fig. 1), it is assumed that the array consists of N smooth surfaced subcollectors

Table 1
Array configurations studied

Configuration	Arrangement of subcollectors in the array
Basic	N smooth surfaced subcollectors of equal duct height in parallel with the same mass flow rate through all the subcollectors.
A	N subcollectors with subcollector 1 having smaller than the nominal duct height ($H_1 < H$) and poorly finished surface, while the remaining subcollectors having duct height larger than the nominal value ($H_i > H$, where $i = 2 - N$).
B	N subcollectors with one of the subcollectors having smaller than the nominal duct height (say, $H_1 < H$) and poorly finished surface. Another subcollector in the array having duct height larger than the nominal value (say, $H_2 > H$), while remaining subcollectors not affected.
C	A poorly manufactured array with one-third or half of the subcollectors having smaller than nominal duct height and the remaining subcollectors having larger than the nominal duct height.

of equal duct height in parallel and, hence, the flow maldistribution will not be present. Since the manifold-induced flow maldistribution has not been considered as stated earlier, the manifolds have not been included in the figure.

While the basic configuration has no manufacturing imperfections, the configurations A–C have different degrees of these imperfections. In the case of configuration A, it has been assumed that duct height of one of the subcollectors in the array of N subcollectors, say subcollector no. 1 in Fig. 1, is smaller by 10% (the assumed tolerance) from the nominal duct height ($H_1 < H$) with a surface finish corresponding to commercial grade, as discussed earlier. Hence, the flow rate through the subcollector 1 will be lower than the nominal value, which is assumed to be compensated by an equal increase in the flow rate through the remaining subcollectors in the array having duct heights larger than the nominal value ($H_i > H$, where $i = 2 - N$).

In the configuration B, the subcollector 1 experiences a reduction in the flow (because of $H_1 < H$ by 10% and commercial grade finish), which is compensated by an increase in the flow through another subcollector in the array while the remaining subcollectors in the array are unaffected. Configurations A and B can be termed as N-passage models. For the analysis, it has been assumed that these configurations are having 10 subcollectors in parallel, i.e., $N = 10$.

The configuration C is a poorly manufactured array. It is a two-passage model as termed by Shah and Sekulic [7] for compact heat exchangers; in this model 50% of the ducts are small ($H_1 < H$ by 10%) and 50% of the ducts are large ($H_2 > H$). The subcollectors with poor surface finish and duct height smaller than nominal will experience a reduction in the flow, and the remaining subcollectors accommodate the reduced flow equally (their duct heights are large compared to the nominal values).

For the configurations A–C, the total flow rate through the array has been kept equal to the basic configuration. Thus the nominal value of G for the array is the same for all configurations and this allows use of G as a common parameter for comparison and presentation of the results. The condition of the equal flow rate for the array has been achieved by allowing an increase in the duct height of a subcollector or the subcollectors accommodating the reduced flow as discussed above. The required duct height for the accommodation of the increased flow has been determined by increasing the duct height in small steps from the nominal value till the condition of equal pressure drop is satisfied. Since the variation in the duct height has been allowed only within the limit of the assumed manufacturing tolerance of 10%, it was found that at the higher flow rates of the study the reduced flow in one subcollector could be accommodated in two subcollectors instead of one in the case of configuration B. Similar was the observation in the case of configuration C.

The nominal value of the air flow rate, ambient temperature, solar insolation, and the wind heat transfer coefficient have been systematically varied within the range of study. The collector length, duct height, and the plate emissivity were also changed to study their effect. The analysis shows that, for all the combinations of these parameters, the reduction in the thermal efficiency of the array, due to the flow maldistribution, is the highest for the configuration C. Hence, the results are being presented for this configuration only. The effect of flow maldistribution is seen to be the lowest for the configuration A, while the results for the configuration B lie in between.

The study shows that at the maximum flow rate of $G = 0.06\,\mathrm{kg\,s^{-1}\,m^{-2}}$, the combined effect of 10% decrease in the duct height and increase in the friction factor due to the duct wall roughness leads to about 20% reduction in the flow through a subcollector. At $G = 0.005\,\mathrm{kg\,s^{-1}\,m^{-2}}$, the reduction in flow is as much as 28%. It must be noted that at the lowest flow rate, the flow is in the laminar regime and the friction factor is not affected due to the duct wall roughness. The decrease in the flow rate in this regime is due to the decrease in the height of the duct only as explained earlier. The observed reduction in flow values can be readily confirmed by approximate transformation of Eq. (2) in terms of flow rate and duct height. For example, in the laminar regime, let $f \approx 24/Re$, which gives $\delta p \propto G/H^3$ when Re is replaced by $2GL/\mu$ for the solar air heater duct [3]. Thus a 10% reduction in H will cause the flow rate to reduce to 0.73 of the nominal value for a specified δp. In the transitional and turbulent flow regime, let the friction factor be approximated by the Blasius equation so that $f \propto Re^{-0.25}$. Considering a 10% enhancement in the friction factor due to the surface roughness at the Reynolds number corresponding to $G = 0.06\,\mathrm{kg\,s^{-1}\,m^{-2}}$, the transformation of the pressure loss equation relative to a smooth duct gives $\delta p \propto 1.1(G^{1.75}/H^3)$. The reduction in the

flow compared to a smooth surfaced subcollector can be seen to be about 20% for the subcollector with commercial grade finish of the duct surface and 10% reduction in the duct height from the nominal value.

The drop in the thermal efficiency of the array due to the flow maldistribution has been presented as relative drop in thermal efficiency ($\Delta\eta/\eta$), which is defined as

$$\Delta\eta/\eta = 1 - \eta_e/\eta, \tag{26}$$

where η_e is the effective efficiency of the array when flow maldistribution is present, and η is the reference or nominal efficiency, which is the efficiency of the basic configuration.

Results showing the effect of change of parameters I, T_a, h_w, β, H, and ε_p on the loss in thermal efficiency of configuration C of 2 m length are presented in Table 2. One parameter has been changed at a time from $I = 1000\,W\,m^{-2}$, $T_a = 313\,K$, $h_w = 50\,W\,m^{-2}\,K^{-1}$, $\beta = 0^\circ$, $H = 10\,mm$ and $\varepsilon_p = 0.95$. It can be seen that the effect of the change of slope from 0° to 45° is negligible.

The results presented in this study are based on the assumption of the sky temperature $T_s = 0.0552T_a^{1.5}$. However, some results were also taken for the assumption of $T_s = T_a$, and the effect on the end result was found to be negligible.

For the duct height of $H = 20\,mm$, the relative drop in efficiency of the array due to the flow maldistribution is found to be moderate (about 1.0–1.5%) over the whole range of the flow rate, which is lower than that for $H = 10\,mm$ at the lowest flow rate but slightly higher at the higher flow rates. However, it must be noted that smaller values of duct height are favoured for high thermal efficiency of collectors. For example, it was found that thermal efficiency of a 2 m long collector with duct height of 20 mm is 11–21% lower than that of a collector with 10 mm duct height depending on the flow rate; the greater effect is experienced at the lowest flow rate.

The relative loss in the thermal efficiency of the array is higher for the higher values of solar insolation, ambient temperature, and wind heat transfer coefficient. It can also be seen from the results presented in Table 2 that an array consisting of subcollectors with a selective coating on the absorber plate is somewhat less affected by the flow maldistribution.

It has been found that the deterioration of the performance of the array is the highest for a horizontally installed array with black painted absorber plate ($\varepsilon_p = 0.95$), when the solar insolation, wind heat transfer coefficient, and the ambient temperature are at their maximum.

From the above discussion it follows that, in the range of present study, combination of $I = 1000\,W\,m^{-2}$, $T_a = 313\,K$, $h_w = 50\,W\,m^{-2}\,K^{-1}$, $\beta = 0^\circ$, $H = 10\,mm$, and $\varepsilon_p = 0.95$ will lead to the highest loss in the efficiency of the array at any mass flow rate. Hence, the plots of Fig. 3 (where the results are presented in the form of plots of the relative drop in thermal efficiency of the array, $\Delta\eta/\eta$, versus the nominal flow rate, G) depict the upper limit of the loss in the thermal efficiency of the array due to the flow maldistribution. The maldistribution results in 0.15–3% reduction in the thermal efficiency of the array depending on the flow rate and length of the array as can be seen in the figure. At the nominal values of flow rate corresponding to the transition and turbulent flow regimes, the loss in the thermal efficiency of the array is less than

Table 2
Effect of change of parameters on the loss in thermal efficiency of array (configuration C, $L = 2\,m$); one parameter has been changed at a time from $I = 1000\,W\,m^{-2}$, $T_a = 313\,K$, $h_w = 50\,W\,m^{-2}\,K^{-1}$, $\beta = 0^\circ$, $H = 10\,mm$ and $\varepsilon_p = 0.95$

1. Solar insolation

G ($kg\,s^{-1}\,m^{-2}$)	I ($W\,m^{-2}$)	$\Delta\eta/\eta$ (%)
0.005	1000	2.43
	500	2.07
0.05	1000	0.87
	500	0.75

2. Ambient temperature

G ($kg\,s^{-1}\,m^{-2}$)	T_a (K)	$\Delta\eta/\eta$ (%)
0.005	313	2.43
	283	2.35
0.05	313	0.87
	283	0.68

3. Wind heat transfer coefficient

G ($kg\,s^{-1}\,m^{-2}$)	h_w ($W\,m^{-2}\,K^{-1}$)	$\Delta\eta/\eta$ (%)
0.005	50	2.43
	5	2.24
0.05	50	0.87
	5	0.65

4. Collector slope

G ($kg\,s^{-1}\,m^{-2}$)	β (deg)	$\Delta\eta/\eta$ (%)
0.005	0	2.43
	45	2.416
0.05	0	0.87
	45	0.846

5. Duct height

G ($kg\,s^{-1}\,m^{-2}$)	H (mm)	$\Delta\eta/\eta$ (%)
0.005	10	2.43
	20	1.31
0.05	10	0.87
	20	1.04

6. Emissivity of plate

G ($kg\,s^{-1}\,m^{-2}$)	ε_p	$\Delta\eta/\eta$ (%)
0.005	0.95	2.43
	0.1	2.25
0.05	0.95	0.87
	0.1	0.52

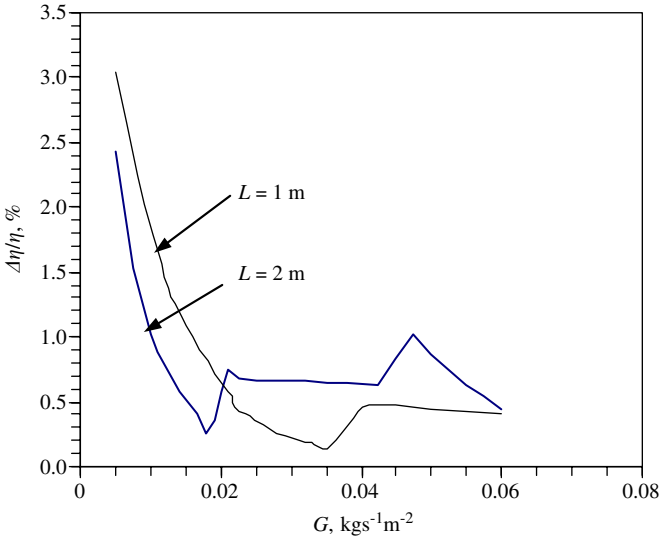

Fig. 3. Loss in thermal efficiency versus the nominal flow rate per unit area of plate ($I = 1000\,\mathrm{W\,m^{-2}}$, $T_a = 313\,\mathrm{K}$, $h_w = 50\,\mathrm{W\,m^{-2}\,K^{-1}}$, $\beta = 0^\circ$, and $\varepsilon_p = 0.95$; $H = 10\,\mathrm{mm}$ for $L = 2\,\mathrm{m}$, and 5 mm for $L = 1\,\mathrm{m}$).

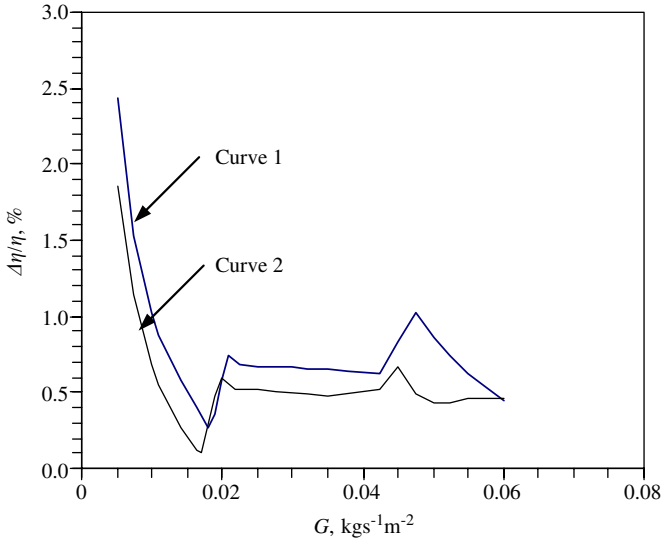

Fig. 4. Effect of insolation and ambient conditions on the loss in thermal efficiency ($L = 2\,\mathrm{m}$, $H = 10\,\mathrm{mm}$, and $\varepsilon_p = 0.95$). Curve 1: $I = 1000\,\mathrm{W\,m^{-2}}$, $T_a = 313\,\mathrm{K}$, $h_w = 50\,\mathrm{W\,m^{-2}\,K^{-1}}$. Curve 2: $I = 500\,\mathrm{W\,m^{-2}}$, $T_a = 298\,\mathrm{K}$, $h_w = 5\,\mathrm{W\,m^{-2}\,K^{-1}}$.

1%. The maximum reduction in efficiency of about 3% is seen to be at the lowest flow rate for the array of 1 m length. It is to be noted that the Reynolds number for the rectangular duct of a solar air heater can be expressed in terms of G and collector length L as $Re = 2GL/\mu$ [3]. This explains the reason for the shift of the curve for $L = 1\,\mathrm{m}$ array to the right with respect to that for $L = 2\,\mathrm{m}$ array in Fig. 3.

Lower values of the solar insolation, wind heat transfer coefficient, and ambient temperature result in a lower loss in the thermal efficiency of the array as seen in Fig. 4 where the effect of insolation and ambient conditions on the relative drop in efficiency has been shown for the fixed values of $L = 2\,\mathrm{m}$, $H = 10\,\mathrm{mm}$, and $\varepsilon_p = 0.95$.

It is seen from Figs. 3 and 4 that the relative drop in the thermal efficiency of the array is lower at the higher flow rates. In general, the efficiency of a solar collector increases with the increase in the flow rate. However, the loss in the thermal efficiency of the array due to the flow maldistribution is relatively lower at higher flow rates. Hence, the relative drop in the efficiency of the array decreases with the increase in the mass flow rate.

The reduction in the efficiency due to the flow maldistribution can be attributed to the fact that the negative effect of lower than nominal flow rates experienced in some of the subcollectors is more than the positive effect of flows equally higher than the nominal in the other subcollectors of the array. This behaviour can be readily explained from the decreasing slope of the efficiency plots with increase in the flow rate in Fig. 5. For example, it was found that, in case of the 2 m array, the reduction in the flow through a subcollector from the nominal value of $G = 0.005\,\mathrm{kg\,s^{-1}\,m^{-2}}$ caused 20% reduction in the thermal efficiency of that subcollector, while an equal increase in the flow rate through another subcollector in the array

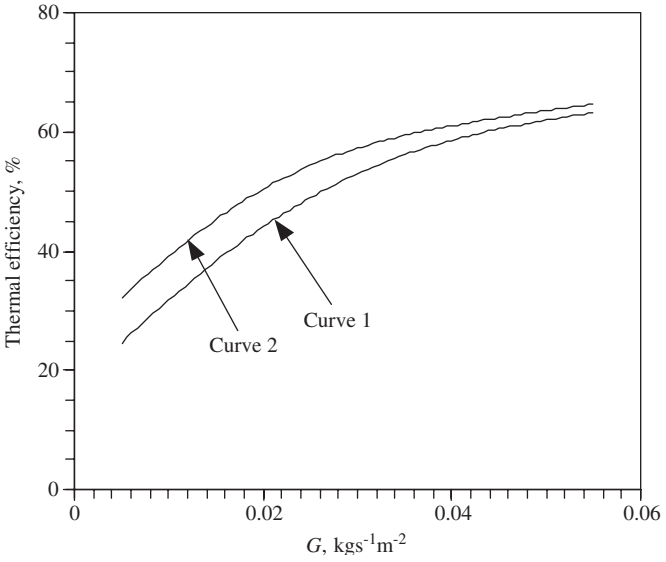

Fig. 5. Variation of thermal efficiency with nominal flow rate per unit area ($L = 2\,\mathrm{m}$, $H = 10\,\mathrm{mm}$, and $\varepsilon_p = 0.95$). Curve 1: $I = 1000\,\mathrm{W\,m^{-2}}$, $T_a = 313\,\mathrm{K}$, $h_w = 50\,\mathrm{W\,m^{-2}\,K^{-1}}$. Curve 2: $I = 500\,\mathrm{W\,m^{-2}}$, $T_a = 298\,\mathrm{K}$, $h_w = 5\,\mathrm{W\,m^{-2}\,K^{-1}}$.

increased the efficiency of this subcollector by 11.1% only. At the higher flow rates, these changes in the efficiency have been found to be lower because of the decreasing slope of the curve at higher flow rates. This explains the reason for the lower relative drop in efficiency at higher values of G seen in Figs. 3 and 4. The smaller slope of the curve 2 (for the combination of lower values of the solar insolation, wind heat transfer coefficient, and the ambient temperature) as compared to that for curve 1 in Fig. 5 explains the reason for the lower loss in thermal efficiency seen for the operational conditions represented by curve 2

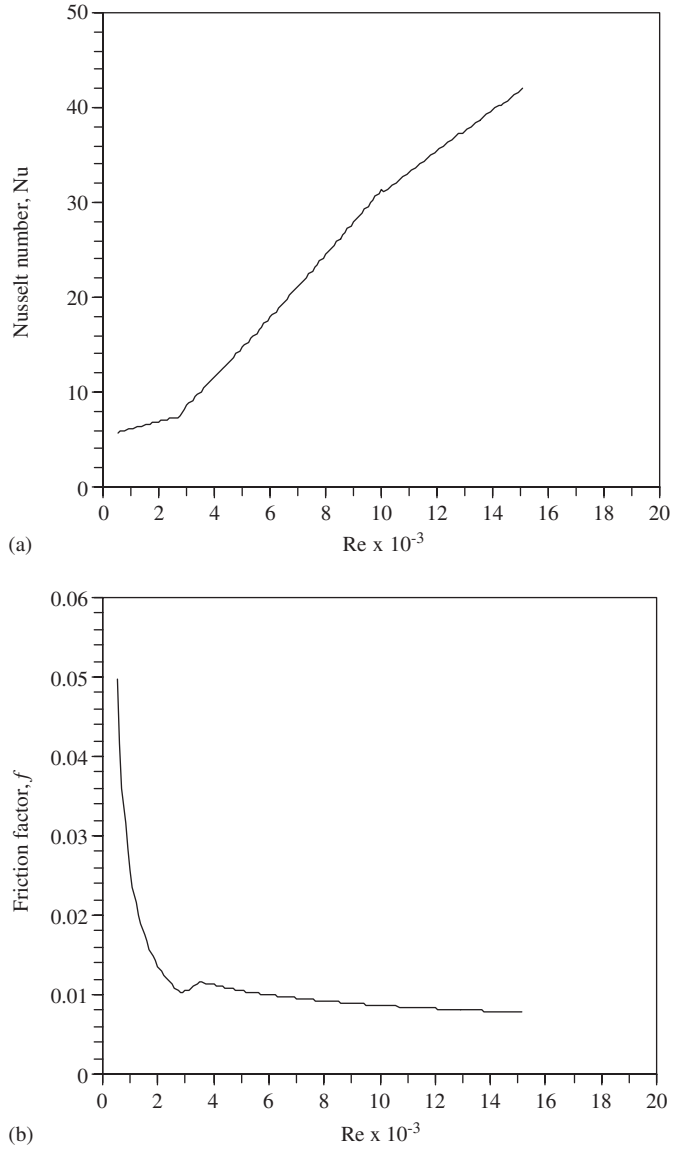

Fig. 6. (a) Nusselt number versus the Reynolds number, and (b) friction factor versus the Reynolds number.

in Fig. 4. From the above observation it can be concluded that a high efficiency collector will be less affected by the flow maldistribution.

The drastic changes in the plots of Figs. 3 and 4 are observed at the junctions of the laminar–transient and transient–turbulent regimes. These changes correspond to the changes in the plots of the Nusselt number and friction factor values from the correlations used in the study as seen in Fig. 6.

A collector array in actual operation will experience varying operating conditions. Ambient temperature varies during the day as well as during the year. The wind does not blow always at its maximum. Hence, the wind heat transfer coefficient will be varying in the range of 5–50 $W m^{-2} K^{-1}$. The solar insolation increases from about 500 $W m^{-2}$ at 9 a.m. to about 1000 $W m^{-2}$ at the solar noon and then again decreases. The desired temperature of the heated air depends not only on the application but also on the ambient conditions. An array in practice may be better than configuration C, which represents a poorly manufactured array. Hence, it can be concluded that the plots in Fig. 3, which are for the configuration C under the worst combination of the operating parameters, represent the upper bound.

From a designer's point of view, it can be recommended from the present study that a properly manufactured solar air heater array (tolerance of $\pm 10\%$ in the height of parallel ducts, and their surface finish ranging from smooth to commercial grade or the finishes of parallel ducts in terms of relative roughness differ by less than 0.002) will experience only a marginal reduction in the thermal efficiency due to the flow maldistribution in the actual operation. Further it is to add that to avoid manifold-induced flow maldistribution, the pressure drop in the collector ducts must be large relative to that in the manifolds.

4. Conclusions

A theoretical study has been carried out to investigate the effect of flow maldistribution, caused by the manufacturing imperfections and tolerances, on the thermal efficiency of a solar air heater array with the subcollectors in parallel.

The flow maldistribution has been found to reduce the thermal efficiency of the array by 0.15–3% depending on the flow rate and combination of various parameters. The maximum reduction in the efficiency is found to be at the lowest flow rate of the study for the array of 1 m length with black painted absorber plate and installed horizontal, when the solar insolation, wind heat transfer coefficient and the ambient temperature are at their maximum. The reduction in the thermal efficiency of the array is less than 1% for the nominal values of mass flow rate corresponding to the transition and turbulent flow regimes. Lower values of solar insolation, wind heat transfer coefficient and ambient temperature result in a lower loss in the thermal efficiency of the array. An array consisting of subcollectors with selective coating on the absorber plate is somewhat less affected by the flow maldistribution. In actual operation, due to the variable operating conditions, the reduction in the thermal efficiency of the array will be lower than the maximum of 3%.

It is concluded that a properly manufactured solar collector array will experience only a marginal reduction in the thermal efficiency due to the flow maldistribution.

References

[1] Yeh HM, Lin TT. Solar air heater with two collectors in series. Energy 1997;22(9):933–9.
[2] Garg HP, Adhikari RS. Model calculation on the performance of a solar air heater with *n*-subcollectors in series configuration.

In: Sawhney RL, Buddhi D, Gautam RP, editors. Proceedings of the 23rd national renewable energy convention '99, December 20–22, 1999, Devi Ahilya Vishwavidyalaya, Indore, India, 1999. p. 240–3.

[3] Karwa R, Garg SN, Arya AK. Thermo-hydraulic performance of a solar air heater with *n*-subcollectors in series and parallel configuration. Energy 2002;27:807–12.

[4] Jones GF, Lior N. Conjugate heat transfer and flow distribution in an assembly of manifolded finned tubes. In: Kitto Jr JB, Robertson JM, editors. Maldistribution of flow and its effect on heat exchanger performance, ASME HTD, vol. 75, 1987. p. 127–36.

[5] Jones GF, Lior N. Flow distribution in manifolded solar collectors with negligible buoyancy effects. Sol Energy 1994;52(3): 289–300.

[6] Weitbrecht V, Lehmann D, Richter A. Flow distribution in solar collectors with laminar flow conditions. Sol Energy 2002;73(6): 433–41.

[7] Shah RK, Sekulic DP. Heat exchangers. In: Rohsenow WM, Hartnett JP, Cho YI, editors. Handbook of heat transfer. New York: McGraw-Hill; 1998 [Chapter 17].

[8] Menuchin Y, Bassler S, Jones GF, Lior N. Optimal flow configuration in solar collector arrays. In: Proceedings of the annual meeting of the AS/ISES, Philadelphia, PA, May 1981. p. 616–20.

[9] Culham R, Sauer P. The effects of unbalanced flow on the thermal performance of collector arrays. J Sol Energy Eng 1984;106:165–70.

[10] Hollands KGT, Shewen EC. Optimization of flow passage geometry for air-heating, plate-type solar collectors. J Sol Energy Eng 1981;103:323–30.

[11] Bhatti MS, Shah RK. Turbulent and transition flow convective heat transfer. In: Kakac S, Shah RK, Aung W, editors. Handbook of single-phase convective heat transfer. New York: Wiley; 1987 [Chapter 4].

[12] Duffie JA, Beckman WA. Solar energy thermal processes. New York: Wiley; 1980. p. 211.

[13] Karwa N, Karwa R. Calculation of top loss coefficient for a flat-plate solar collector with single glass cover. In: Proceedings of the national conference on emerging energy technologies, March 28–29, 2003, NIT, Hamirpur, India, 2003. p. 89–95.

[14] Buchberg H, Catton I, Edwards DK. Natural convection in enclosed spaces—a review of application to solar energy collection. J Heat Transfer 1976:182–8.

[15] Klein SA. Calculation of flat-plate collector loss coefficients. Sol Energy 1975;17:79–80.

[16] Ebadian MA, Dong ZF. Forced convection, internal flow in ducts. In: Rohsenow WM, Hartnett JP, Cho YI, editors. Handbook of heat transfer. New York: McGraw-Hill; 1998 [Chapter 5].

[17] Heaton HS, Reynolds WC, Kays WM. Heat transfer in annular passages. Simultaneous development of velocity and temperature fields in laminar flow. Int J Heat Mass Transfer 1964;7:763–81.

[18] Kays WM, Perkins HC. Forced convection, internal flows in ducts. In: Rohsenow WM, Hartnett JP, editors. Handbook of heat transfer. New York: McGraw-Hill; 1973 [Chapter 7].

[19] Lee Y. Turbulent heat transfer from the core tube in thermal entrance regions of concentric annuli. Int J Heat Mass Transfer 1968;11: 509–22.

[20] Barrow H, Lee Y. Heat transfer with unsymmetrical thermal boundary conditions. Int J Heat Mass Transfer 1964;7:580–2.

[21] Kays WM, Leung EY. Heat transfer in annular passages- hydrodynamically developed turbulent flow with arbitrarily prescribed heat flux. Int J Heat Mass Transfer 1963;6:537–57.

[22] Kays WM, Crawford ME. Convective heat and mass transfer. New Delhi: Tata McGraw-Hill Publishing Co.; 1983.

[23] Tan HM, Charters WWS. An experimental investigation of forced-convective heat transfer for fully developed turbulent flow in rectangular duct with asymmetric heating. Sol Energy 1970;13:121–5.

[24] Hatton AP, Quarmby A, Grundy I. Further calculations on the heat transfer with turbulent flow between parallel plates. Int J Heat Mass Transfer 1964;7:817–23.

[25] Sparrow EM, Lloyd JR, Hixon CW. Experiments on turbulent heat transfer in an asymmetrically heated rectangular duct. J Heat Transfer 1966;May:170–4.

[26] Kays WM, London AL. Compact heat exchangers. New York: McGraw-Hill; 1964.

[27] Niles PW, Carnegie EJ, Pohl JG, Cherne JM. Design and performance of an air collector for industrial crop dehydration. Sol Energy 1978;20:19–23.

[28] Swinbank WC. Long-wave radiation from clear skies. Q J Roy Meteor Soc 1963;89:339.

[29] Karwa R, Solanki SC, Saini JS. Thermo-hydraulic performance of solar air heaters having integral chamfered rib roughness on absorber plates. Energy 2001;26(2):161–76.